A D-Band 13-mW Dual-Mode CMOS LNA for Joint Radar–Communication in 22-nm FD-SOI CMOS

Shankkar Balasubramanian, *Graduate Student Member, IEEE*, Kristof Vaesen, *Member, IEEE*, Anirudh Kankuppe, *Member, IEEE*, Sehoon Park, *Member, IEEE*, and Carsten Wulff, *Member, IEEE*

***Abstract*—This letter presents a D-band low-noise amplifier (LNA) for joint radar–communication applications in 22-nm CMOS technology. The 4-stage LNA uses transistor switching and bias class changes to achieve dual-mode functionality. In the radar mode, the LNA achieves gain of 17 dB, noise figure (NF) of 7.7 dB, 3-dB bandwidth (BW) of 117–129 GHz, and IP_{1dB} of −20 dBm, respectively. In the communication mode, the LNA achieves gain of 22.6 dB, NF of 8.5 dB, BW of 115.9–128.9 GHz, and IP_{1dB} of −29 dBm, respectively. The power consumption for the radar and communication modes is 13 and 12.2 mW, respectively. The LNA has a core area of 0.06 mm^2.**

***Index Terms*—CMOS, communication, D-band, gain boosting, low-noise amplifiers (LNAs), mm-wave, radar.**

I. Introduction

LARGE available bandwidth (BW) in the D-band (110–170 GHz) favors high-resolution radar systems and next-generation high data rate communication systems. Spectrum sharing in beyond-5G systems allows both systems to use the same radio frequency blocks. In addition, the two systems have the potential to help each other to increase the operational efficiency of the product. For example, radar sensing can help in accurate beamforming during communication, while the communication subsystem can facilitate radar data exchange between sensors [1].

Receivers (RXs) for communication and radar have conflicting requirements [2]. In a full-duplex radar, the RX must tolerate high transmitter (TX) to RX leakage. Thus, high IP_{1dB} is prioritized over gain, noise figure (NF), and power consumption. Simplex communication RX, on the other hand receives low signal power at D-band which relaxes the IP_{1dB} requirement. As a result, RX front-end in communication mode can be optimized for lower power consumption, better gain, and NF. Hence, the RX front-end must be programmable to support the two systems to save chip area.

Fusion between the two systems is a relatively new concept in the D-band frequencies. Mixer-first architectures are preferred for high IP_{1dB} [3], but due to the high NF, RX sensitivity is degraded. In another case, supply switching is used after downconverting to the first intermediate frequency (IF) to facilitate different filtering and BW requirements for radar and communication, while the low-noise amplifier (LNA) is the same for both systems [4]. In [5], 2-stage CS-LNA is demonstrated, which has good gain and NF, but not a high IP_{1dB}.

The prior art cannot be effectively used for a joint radar–communication system as it lacks programmability in the front end. In this letter, a programmable-gain LNA suited for joint radar–communication applications is demonstrated.

Manuscript received 1 July 2024; revised 21 August 2024 and 2 September 2024; accepted 2 September 2024. Date of publication 9 September 2024; date of current version 17 September 2024. This work was supported by the Research Council of Norway under Project 321204. This article was approved by Associate Editor Yunzhi Dong. *(Corresponding author: Shankkar Balasubramanian.)*

Shankkar Balasubramanian and Carsten Wulff are with the IC Development, Nordic Semiconductor ASA, 7052 Trondheim, Norway, and also with the Department of Electronic Systems, Norwegian University of Science and Technology, 7034 Trondheim, Norway (e-mail: shankkar.balasubramanian@ntnu.no).

Kristof Vaesen and Anirudh Kankuppe are with IMEC, 3001 Leuven, Belgium.

Sehoon Park is with the School of Electronic and Electrical Engineering, Kyungpook National University, Daegu 41566, South Korea.

Digital Object Identifier 10.1109/LSSC.2024.3455889

II. Circuit Design

A. LNA Stages

The architecture of the LNA is shown in Fig. 1(a). The LNA has four common source (CS) stages. In both modes (radar and communication), the input stage is designed for optimized NF and gain while dual-mode functionality is achieved by varying bias currents in the second and third stages (STG2, STG3), and switchable transistors in the last stage (STG4). In the communication mode, the stages are biased with a current density of 0.15 mA/μm, based on the tradeoff between power consumption, NF and gain. In the radar mode, the first and last stages retain the previous current density, while the middle stages are biased in Class-B mode where gain is lowered to get higher IP_{1dB}. For all the stages, capacitive neutralization boosts the gain, while maintaining the stability factor (K_f) around 1.6 before including the loss of matching networks. It also allows for simultaneous noise and gain matching by bringing the available gain and noise circles closer to each other [6]. The f_{max} and G_{max} at 140 GHz of the neutralized differential amplifier in STG1–3 are 280 GHz and 9.2 dB, respectively.

B. Programmability for Joint Radar–Communication

In the radar mode, we assume a state-of-the-art D-band PA with output power of 13 dBm [4] along with a measured TX-RX isolation of 37 dB [7], which results in the minimum IP_{1dB} specification of −24 dBm. The higher IP_{1dB} of radar mode requires a large width transistor in the last stage (STG4) which results in increased power consumption. In the communication mode, the required IP_{1dB} is lower, hence a smaller width transistor is sufficient. When operating in communication mode, power can be saved by switching to a smaller overall transistor width in the last stage which is achieved by combination of M_{R1} and M_{R2} and switches SW1 and SW2 as shown in Fig. 2. During the radar mode, nodes A and B are shorted to the gates of M_{C1} and M_{C2}, respectively, doubling the overall

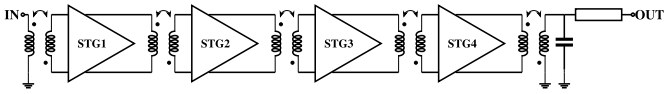

	Pdc (mW)				
Mode	TOT	STG1	STG2	STG3	STG4
Comm.	11.6	2.9	2.9	2.9	2.9
Radar	11.5	2.9	2.1	0.7	5.8

(a)

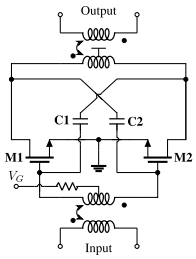

M1,M2	12 μm/ 18 nm	C1,C2	3.5 fF

(b)

Fig. 1. (a) Block diagram of LNA along with the simulated power consumption of each stage in the two modes. (b) CS stage with capacitive neutralization for STG1–3.

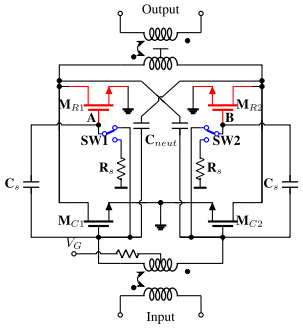

M_{R1},M_{R1}	12 μm/ 18 nm	C_s	40 fF
M_{C1},M_{C2}	12 μm/ 18 nm	C_{neut}	7.6 fF
		R_s	38 kΩ

Fig. 2. STG4 circuit diagram in radar mode.

width of the STG4 transistors which in-turn boosts the output compression power of the LNA. In the communication mode, nodes A and B are shorted to ground halving the overall width and reducing the current consumption. C_s isolates the bias voltages of gates of active M_{C1}(M_{C2}) and grounded M_{R1}(M_{R2}). In comparison to the STG1, an extra loss of 1.3 dB is introduced to the communication mode due to loss of RF energy through C_s resulting in higher NF_{min} of STG4. But, the overall NF of the LNA is not significantly affected in communication mode thanks to the higher gain of the preceding stages. The simulated NF of LNA in communication mode is 0.3 dB better than the radar mode.

Simulated G_{max} and stability factor (K_f) in the two modes for STG4 as a function of neutralization capacitance, C_{neut} are shown in Fig. 3 for two values of C_s. Higher values of isolation capacitance, C_s lead to a higher loss in communication mode whereas the higher C_s increases the gain of LNA in radar mode. Therefore, C_s can be used as a parameter to control the gain of the communication mode. In Fig. 3(a), with C_s

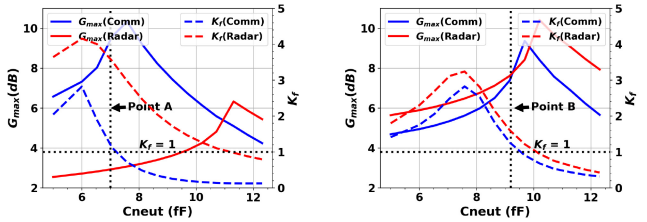

(a) (b)

Fig. 3. G_{max} (continuous line) and K_f (dashed line) in radar and communication modes with sweep of neutralization capacitor, C_{neut} for STG4 with (a) C_s = 0 fF and (b) C_s = 40 fF. With choice of neutralization capacitance as design point A, G_{max} in communication mode is high, but gain in radar mode is low. With choice of neutralization capacitance as design point B, G_{max} in both modes is simultaneously high. Therefore, B is a better design point for dual-mode operation.

= 0 fF, the G_{max} is low for STG4 in the radar mode. This implies that the gain in the radar mode needs to be derived from the earlier stages. As a result, the current consumption of the LNA is increased. Furthermore, the earlier stages become the bottleneck for obtaining a good IP_{1dB}, which results in further increase of power consumption. Therefore, the gain in STG4 in radar mode cannot be very low. With a higher choice of C_s as shown in Fig. 3(b), high gain in the radar mode can be achieved at the expense of a slight increase in loss in the communication mode. For the choice of the neutralization capacitance in Fig. 3(b), G_{max} for the two modes are similar. Higher gain can be achieved in the radar mode by increasing the neutralization capacitor further, but it degrades the IP_{1dB} in the radar mode as well as create instability in the communication mode. The operating gains of STG4 for the communication and radar modes are 6.1 and 7.1 dB, respectively. The difference of 1 dB can be interpreted as the loss associated with communication mode to facilitate dual-mode operation.

This dual-mode functionality does not affect the matching insertion loss significantly. The input shunt resistance of STG4 changes from 450 to 350 Ω, while the shunt capacitance changes by about 3% for the two modes. The simulated change in matching network insertion loss is 0.2 dB. The output resistances are 450 and 900 Ω for the radar and communication modes, respectively. The impedance transformation ratio to 50 Ω is high in both cases. Therefore, the insertion loss difference is less than 0.1 dB for the two modes.

In addition to programmability in the last stage, biasing plays an important role to improve IP_{1dB} in the radar mode. STG1 biasing is kept same as in communication mode to maintain the same optimum input and noise match conditions. Increasing the current density in STG4 improves OP_{1dB} negligibly, and the gain increase results in worse IP_{1dB}. Therefore, only the biasing in the middle stages (STG2, STG3) is changed in the radar mode. The desired power gain is decided by the NF specification of the receiver, and the NF of the mixer and IF chain. Fig. 4 shows that the output compression point, OP_{1dB}, of the LNA in radar mode varies by about 2 dB with sweep of bias of STG2 and STG3. The power gains of the LNA in the plot are in the range of 14–16 dB. The best OP_{1dB} is obtained for the case of low current density in STG3 highlighting the effect of gain

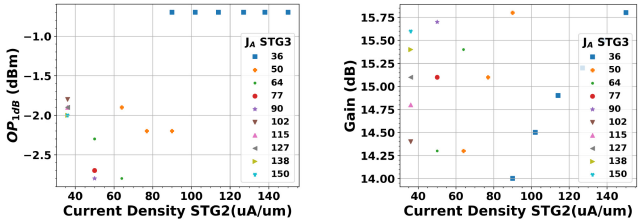

Fig. 4. (a) Simulated 1-dB output compression point (OP_{1dB}) with sweep of bias of STG2 and STG3 when the gain of LNA is between 14 and 16 dB, and (b) corresponding gain. The label "J_A STG3" denotes the current density of STG3 in $\mu A/\mu m$.

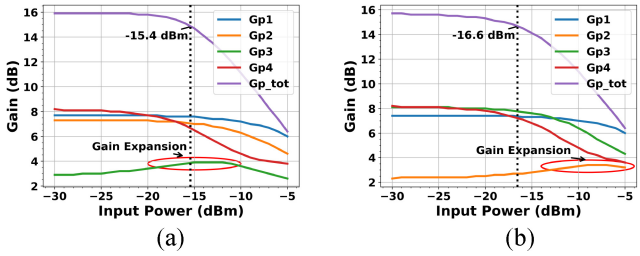

Fig. 5. (a) Operating power gains of the stages (Gp1–4) when STG3 is biased in class-B in radar mode. (b) Operating power gains of the stages when STG2 is biased in class-B in radar mode. Other stages are kept at same current density as in communication mode. Gp_tot is the total power gain of LNA.

expansion on improvement in compression point. Fig. 5 shows the reason why having STG3 in class-B biasing shows better OP_{1dB} than the case when STG2 is in class-B biasing for the same gain in this implementation. The gain expansion in STG3 coincides with start of compression of STG4 in Fig. 5(a), and thus gives better OP_{1dB} performance for the LNA. The gain expansion gives more improvement in IP_{1dB} than the decrease in gain. Overall, the power consumption of LNA in the radar mode is comparable to the communication mode. Though the doubling of the transistor width in STG4 increases the power consumption, it is compensated by the decrease in power consumption in the middle stages. The power consumption of the LNA is 11.6 mW in the communication mode and 11.5 mW in the radar mode. Fig. 1(a) shows the simulated power consumption breakdown for the two modes. The simulated gains at 140 GHz for LNA in communication and radar modes are 19.2 and 14.4 dB, respectively, while the IP_{1dB} are -22.7 and -14 dBm. The improvement in IP_{1dB} is 8.7 dB, while the decrease in gain is 4.8 dB, highlighting the impact of transistor switching and bias change of middle stages in the radar mode.

C. Matching Networks

The interstage matching is achieved using low-k transformers designed as fourth-order filters [8]. The coupling factor for the interstage matching transformer is 0.21. The maximum power loss in interstage matching networks is 2.1 dB. The input matching network for the LNA uses a high-k transformer, for optimum noise and input matching. The output matching to 50 Ω is achieved with a balun, shunt capacitor and a single-ended transmission line yielding an insertion loss of 2.8 dB.

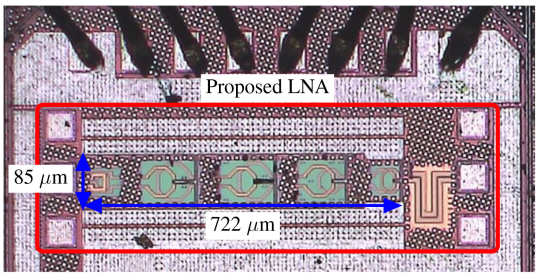

Fig. 6. Chip micrograph of the proposed LNAs.

The simulated fractional BWs for communication and radar modes are 15% and 18.5%, respectively.

III. Measurements

The chip micrograph of Fig. 6 shows the proposed dual-mode LNA fabricated in a 22-nm CMOS FDSOI process. The chip size is 1 mm^2 with core area of 0.06 mm^2.

The S-parameters of the LNA are measured using N5247B PNA-X including extenders from VDI (WR6.5-VNAX). Infinity Waveguide Probes from FormFactor are used for probing on the on-chip GSG pads. The NF is measured using the gain method and the setup includes a low pass filter in addition to the extenders to filter out LO leakage to the network analyzer.

Fig. 7 shows the small signal parameters for the LNA in communication and radar modes. In the communication mode, the peak gain for the LNA is 22.6 dB at 122.7 GHz with a 3-dB BW of 13 GHz. The NF from a polynomial fit of measured points is 8.5 dB at the center, with a minimum NF of 7.8 dB at 129 GHz.

In the radar mode, the peak gain for the LNA is 17 dB at 122.7 GHz with a 3-dB BW of 12 GHz. The NF is 7.7 dB at the center frequency with a minimum NF of 7.4 dB at 127 GHz. The dc power consumption for the two modes from 0.8 V supply is 12.2 and 13 mW, respectively. The gain is 5.6 dB higher in the communication mode, while the NF, BW, and power consumption are similar in both modes.

The LNA is unconditionally stable across the frequency range. The frequency of peak gain is downshifted by approximately 10% compared to simulations, attributed to inaccurate modeling of capacitance in the active devices, and the metal capacitors.

The measured linearity of the LNA at 124 GHz is shown in Fig. 7(c). The LNA shows IP_{1dB} of -28.2 and -19.6 dBm for communication and radar modes with gains of 21.8 and 16 dB, respectively. Even though the gain change is 5.9 dB, the IP_{1dB} improvement is approximately 9 dB, thanks to the transistor switching in the last stage and Class-B driven gain expansion of the middle stages. Fig. 8 shows that the IP_{1dB} improvement is consistent across the measured frequencies. To get better IP_{1dB}, the gains for the radar mode can be lowered further by adjusting the bias points of the middle stages (STG2, STG3). In these high linearity modes, the LNA achieves IP_{1dB} of -16 dBm with gain of 12.5 dB.

This letter is compared with the state-of-the-art LNAs in Table I. For comparing performance of LNAs, a well-known figure of merit, FOM1, is used [7], while FOM2 compares

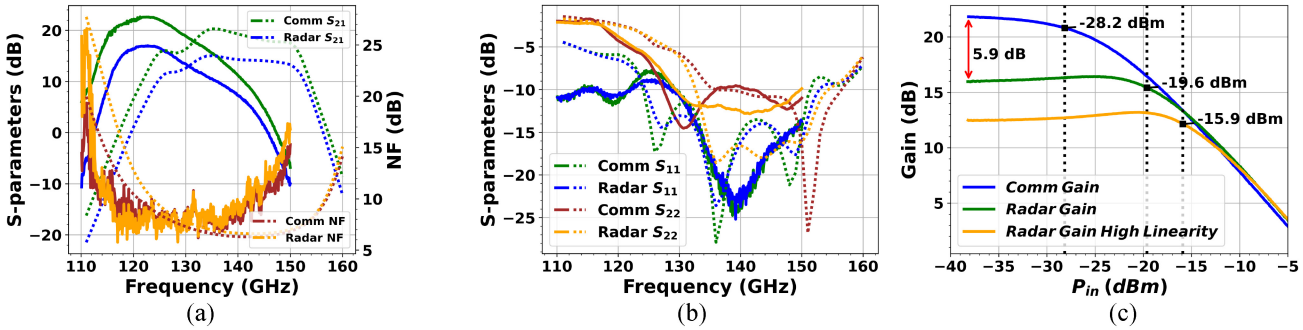

Fig. 7. (a) NF and S_{21} of the proposed LNA. (b) S_{11} and S_{22} of the LNA. Solid line: measurement; dotted line: simulation. (c) Measured large signal performance and IP_{1dB} of the LNA at 124 GHz.

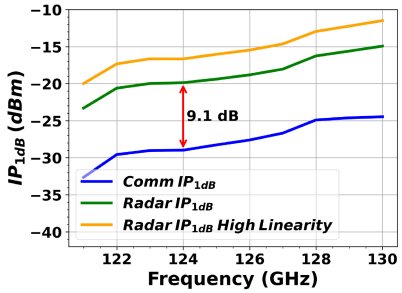

Fig. 8. Measured IP_{1dB} of the LNA across frequency.

TABLE I
PERFORMANCE COMPARISON OF D-BAND LNAS

Ref	This work	[5]	[9]	[10]
Frequency (GHz)	**122.7/122.7**	152.2	135	153
Technology	**22-nm FD-SOI**	65-nm CMOS	40-nm CMOS	40-nm CMOS
Mode/Topology	**Comm/Radar Differential 4 CS**	Single-ended 3 CS	Differential 5 CS	Differential 5 CG
VDD (V)	**0.8**	0.65	0.8	1
3dB-BW (GHz)	**115.9-128.9/ 117-129**	146-157	115.7-139.7	131-162
Peak Gain (dB)	**22.6 / 17**	17.9	19.7	20.9
PDC (mW)	**12.2 / 13**	13.7	17.8	49
NF (dB)	**8.5 / 7.7**	6.2	9	6.2
IP_{1dB}	**-29 / -20**	-23.8	-24.8	-19.5
FOM1 (dB)[1]	**7.5 / 1.4**	6	5.5	6.9
FOM2 (dB)[2]	**-72.8 / -59**	-62.4	-71.8	-62

[1] FOM1 = 20*log(Gain(lin) * 3dB-BW(GHz) /PDC(mW)/(NF(lin)-1)).
[2] FOM2 = 20*log(Gain(lin) * IP_{1dB}(mW) /PDC(mW)/(NF(lin)-1)).
Gain(lin) = $10^{\text{Gain (dB)}/20}$. NF(lin) = $10^{\text{NF (dB)}/10}$. IP_{1dB}(mW) = $10^{\text{IP}_{1dB}\text{ (dBm)}/10}$.

the IP_{1dB} performance of the LNAs as well [9]. The proposed LNA achieves state-of-the-art performance in terms of gain, NF, and power efficiency in communication mode despite the losses associated with the mode switching. The high gain of the LNA in communication mode prevents the degradation of the overall RX NF. In the radar mode, the achieved IP_{1dB} is comparable to the state-of-the-art works with similar gain, with competitive power consumption and NF, showing the advantages of the proposed switching and gain expansion mechanisms.

IV. CONCLUSION

A D-band dual-mode LNA suited for joint communication and radar was demonstrated. This letter shows that using bias changes and transistor switching, it is possible to design LNAs that achieve good NF, high gain, and low power consumption in the communication mode while also achieving good IP_{1dB} performance for the radar mode.

ACKNOWLEDGMENT

The authors would like to thank Koenraad Vanhoutte, Nele Van Hoovels, and Dr. Yang Zhang for technical support and discussions during the research.

REFERENCES

[1] C. De Lima et al., "Convergent communication, sensing and localization in 6G systems: An overview of technologies, opportunities and challenges," *IEEE Access*, vol. 9, pp. 26902–26925, 2021, doi: 10.1109/ACCESS.2021.3053486.
[2] F. Bozorgi, P. Sen, A. N. Barreto, and G. Fettweis, "RF front-end challenges for joint communication and radar sensing," in *Proc. 1st IEEE Int. Online Symp. Joint Commun. Sens. (JC & S)*, 2021, pp. 1–6, doi: 10.1109/JCS52304.2021.9376387.
[3] A. Mostajeran, A. Cathelin, and E. Afshari, "A 170-GHz fully integrated single-chip FMCW imaging radar with 3-D imaging capability," *IEEE J. Solid-State Circuits*, vol. 52, no. 10, pp. 2721–2734, Oct. 2017, doi: 10.1109/JSSC.2017.2725963.
[4] W. Deng et al., "A D-band joint radar-communication CMOS transceiver," *IEEE J. Solid-State Circuits*, vol. 58, no. 2, pp. 411–427, Feb. 2023, doi: 10.1109/JSSC.2022.3185160.
[5] B. Yun, D.-W. Park, H. U. Mahmood, D. Kim, and S.-G. Lee, "A D-band high-gain and low-power LNA in 65-nm CMOS by adopting simultaneous noise- and input-matched G_{max}-core," *IEEE Trans. Microw. Theory Techn.*, vol. 69, no. 5, pp. 2519–2530, May 2021, doi: 10.1109/TMTT.2021.3066972.
[6] X. Tang, J. Nguyen, G. Mangraviti, Z. Zong, and P. Wambacq, "Design and analysis of a 140-GHz T/R front-end module in 22-nm FD-SOI CMOS," *IEEE J. Solid-State Circuits*, vol. 57, no. 5, pp. 1300–1313, May 2022, doi: 10.1109/JSSC.2021.3139359.
[7] A. Visweswaran et al., "A 28-nm-CMOS based 145-GHz FMCW radar: System, circuits, and characterization," *IEEE J. Solid-State Circuits*, vol. 56, no. 7, pp. 1975–1993, Jul. 2021, doi: 10.1109/JSSC.2020.3041153.
[8] M. Vigilante and P. Reynaert, "On the design of wideband transformer-based fourth order matching networks for E-band receivers in 28-nm CMOS," *IEEE J. Solid-State Circuits*, vol. 52, no. 8, pp. 2071–2082, Aug. 2017, doi: 10.1109/JSSC.2017.2690864.
[9] K. Kim, J. Kang, K. Lee, S.-U. Choi, J. Kim, and H.-J. Song, "A 115.7–139.7 GHz amplifier with 19.7 dB peak gain and 7.9 dB NF in 40-nm CMOS," in *Proc. IEEE/MTT-S Int. Microw. Symp.*, 2023, pp. 48–51, doi: 10.1109/IMS37964.2023.10187943.
[10] I. Kim, H. Koo, W. Kim, and S. Hong, "A 131–162-GHz wideband CMOS LNA using asymmetric frequency responses of triple-coupled transformers," *IEEE Microw. Wireless Technol. Lett.*, vol. 33, no. 11, pp. 1544–1547, Nov. 2023, doi: 10.1109/LMWT.2023.3311043.